LINE-OF-SIGHT APPROXIMATION TO THE EQUIVALENCE PRINCIPLE

Nagula Sangary[(1)] and Natalia K. Georgieva[(2)]

[(1)] Research In Motion, 295 Phillip Street, Waterloo, Ontario N2L 3W8, Canada. nsangary@rim.net

[(2)] Department of Electrical and Computer Engineering, McMaster University, 1280 Main Street West, Hamilton, Ontario L8S 4K1, Canada. talia@mcmaster.ca

ABSTRACT

A line-of-sight (LoS) approximation to the equivalence principle used in far-field computations is proposed. In the LoS equivalence, only the surface currents at the virtual surface and the edge currents at its contour, which are on the LoS with the observation point, are used in the calculation of the radiated field. It is a far more efficient alternative to the standard equivalence principle, which requires integration over the entire closed virtual surface. We present the theory associated with the LoS equivalence approach, examine the error due to the approximation, and demonstrate its accuracy via the radiation of a dipole antenna.

INTRODUCTION

The equivalence principle has been widely used in the analysis of the radiation patterns of antennas. It states that an original problem with radiating sources can be transformed into an equivalent problem with equivalent sources on an arbitrary closed surface [1]-[3]. The region of interest in radiation/scattering problems extends to the far zone. It is impossible to accommodate such a region in the computational space of a finite volume numerical technique. With these techniques, the equivalence principle is practically the only means of pattern computations. However, it requires large computational time. In this paper, we introduce an approximation to the standard equivalence principle, namely the line-of-sight (LoS) equivalence approach to far-field computations. It significantly increases the efficiency of the radiation pattern computations when used with numerical techniques such as the finite-difference time domain (FDTD) method.

The LoS approximation to the equivalence principle considers the source contributions from surface currents that are on the LoS surface only; as well as the currents along the LoS contour. The conditions necessary for the validity of the LoS approximation are: (i) the radiating equivalent sources are in free space and field is bounded at infinity, and (ii) the observation point is in the far-field region. For every observation point, the virtual closed surface consists of the LoS surface and the 'shadow' surface (see Fig.1). The 'shadow' surface can be transformed into an infinite surface supported by the LoS contour. Every line, which passes through the observation point and a point on the LoS contour, belongs to this infinite surface (see Fig.1). In our approach, the integration of the equivalent currents on the infinite surface is approximated by a contour integration over the edge currents along the LoS contour.

Over the last half a century, significant attention has been paid to the solutions to diffraction and scattering problems, for example, see [4]-[7]. Most of these references treat the problem of reducing the surface integrals to contour integrals and they are focused mainly on the application to scattering problems. The fundamental difference between a scattering problem and an equivalence problem is that in the former the position vectors of the field on the surface of the scatterer, of the radiating source and of the observer, are known; while in the latter, only two of these position vectors are known: the position vectors of the surface field and of the observer. Therefore, the

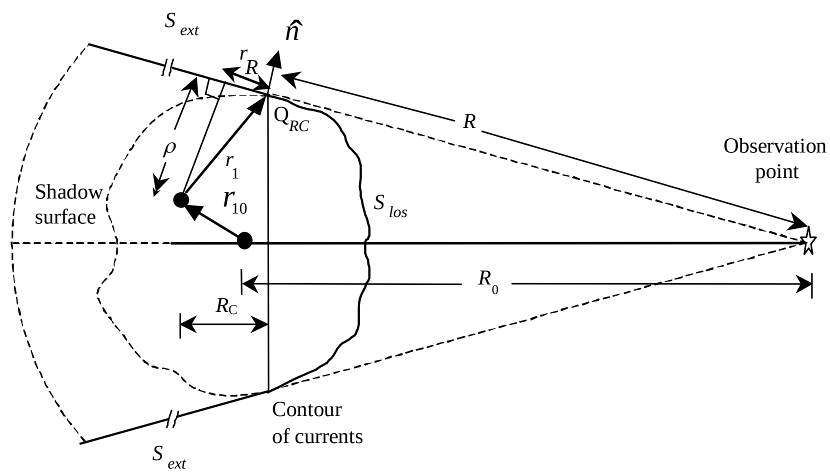

Fig. 1. Equivalent surfaces and LoS approximation notations.

approximate expressions obtained for the scattering problem cannot be applied directly to the equivalence problem. In [6], the Modified Edge Representation (MER) is proposed and the authors derive a general mathematical expression for the surface-to-contour transformation using Stokes theorem. In [6], using field equivalence, an approximate solution is obtained for the surface integral. The derivations in [6] are based on the use of two deformed surfaces (reflection and shadow boundaries), which are needed to obtain near zone accuracies for the diffracted field. Our LoS approximation is developed for far field computations. This allows the shape of the extended surface to be transformed from an infinite conical frustum to an infinite tubular frustum. Unlike in [6], we use an approximation to the open-space potential integral solution rather than diffraction equations such as the Stratton-Chu representation (see [7]). With this approximation, the derivation and implementation of the LoS approach to the radiation problem becomes simple and straightforward.

THEORY

In accordance with the equivalence principle, the time harmonic *E*-field in the far zone can be expressed in terms of the surface electric and magnetic fields $\vec{E}^S$ and $\vec{H}^S$ on the surface enclosing the radiating sources [3]:

$$\vec{E} = -j\omega \iint_S \left(\hat{n}\times\vec{H}^S\right)\frac{e^{-j\beta R}}{R}ds - j\omega\eta \iint_S \left(\hat{R}\times\left(\hat{n}\times\vec{E}^S\right)\right)\frac{e^{-j\beta R}}{R}ds \tag{1}$$

Here, as shown in Fig. 1, R is the distance from the surface field to the observation point, $\hat{n}$ is the unit normal to the surface, $\hat{R}$ is the unit vector from the surface source to the observation point, β is the free-space wave number, ω is the frequency, and η is the free space impedance.

The LoS approximation is obtained by transforming the 'shadow' surface into an infinite (extended) surface supported by the LoS contour, as shown in Fig. 1. When the observation point is in the far zone, the extended surface becomes a semi-infinite tubular frustum surface whose profile is defined by the LoS contour. The far field is calculated from the electric and magnetic surface current density on the LoS surface (S_{los}) and on the extended surface (S_{ext}). In the LoS approach, the current on S_{los} is included in the calculation of the far field. Thus, our objective is to find an approximation to the contribution of the current on S_{ext}. Equation (1) is written as

$$\vec{E}_{MS_{ext}} = -j\omega\eta \iint_{S_{ext}} \hat{R}\times\left(\hat{n}\times\vec{E}^s\right)\frac{e^{-j\beta R}}{R}ds = -j\omega\eta \iint_{S_{ext}} \hat{n}E_R^S\frac{e^{-j\beta R}}{R}ds = -j\omega\eta\oint_C \hat{n}\left[\int_{Q_{RC}}^{+\infty} E_R^S\frac{e^{-j\beta R}}{R}dr_R\right]dl_C \tag{2}$$

In (2), the relation $\hat{n}\cdot\hat{R}=0$ has been used (see Fig. 1). E_R^S is the *R*-component of the electric field on the extended surface, Q_{RC} is a point on the contour *C* and r_R is the distance along the line of sight from the equivalent surface source to the LoS contour.

Similarly, with the far field assumption that the radial field components are negligible, the contribution of the electric surface current density on the extended surface to the field in the far zone is

$$\vec{E}_{JS_{ext}} = -j\omega \iint_{S_{ext}} \left(\hat{n}\times\vec{H}^S\right)\frac{e^{-j\beta R}}{R}ds = -j\omega \iint_{S_{ext}} (-\hat{R}\times\hat{n})H_\tau^S\frac{e^{-j\beta R}}{R}ds = j\omega\oint_C \left(\hat{R}\times\hat{n}\right)\left[\int_{Q_{RC}}^{+\infty} H_\tau^S\frac{e^{-j\beta R}}{R}\,dr_R\right]dl_C \tag{3}$$

where, H_τ^S is the magnetic field component along $\hat{n}\times\hat{R}$.

The approximate solutions to the integrals within the square brackets in (2) and (3) are obtained from the expressions for the surface field components, H_τ^{Se} and E_R^{Se}, which are due to an infinitesimal electric dipole element $I d\vec{l} = I_R\hat{R} + I_\tau\hat{\tau} + I_n\hat{n}$ located at (r_R, r_τ, r_n) [3]:

$$H_\tau^{Se} = \frac{\left(1+j\beta r_1\right)e^{-j\beta r_1}}{4\pi r_1^3}\left(r_n I_R - r_R I_n\right) \tag{4}$$

$$E_R^{Se} = \frac{j\eta e^{-j\beta r_1}}{4\pi\beta r_1^3}\left(-3-3j\beta r_1+\beta^2 r_1^2\right)\frac{r_R}{r_1^2}\left(r_n I_n + r_\tau I_\tau + r_R I_R\right) + \frac{j\eta e^{-j\beta r_1}}{4\pi\beta r_1^3}\left(1+j\beta r_1-\beta^2 r_1^2\right)I_R \tag{5}$$

Here, as shown in Fig. 1, r_1 is the distance between the equivalent surface source and the original source. The total surface field components, H_τ^S and E_R^S, are a superposition of all elemental contributions H_τ^{Se} and E_R^{Se}, respectively.

For the far field approximation, the extended surface is of a tubular shape. The radial distance from the source to the surface of the tube is $\rho = \sqrt{r_1^2 - r_R^2}$, where $r_R = R_0 - R + \left(\vec{r}_{10} \cdot \hat{R}\right)$. In the far zone, the inner integral of (3) over the elemental contribution H_R^{Se} can be written as:

$$\mathcal{J}_H = \int_{r_R(l)}^{-\infty} H_\tau^{Se} \frac{e^{-j\beta R}}{R} dr_R = \frac{e^{-j\beta(R_0+\vec{r}_{10}\cdot\hat{R})}}{R_0} \int_{Q_{RC}}^{-\infty} \tilde{H}_\tau^{Se} e^{-j\beta(r_1-r_R)} \; dr_R \tag{6}$$

where $H_\tau^{Se} = \tilde{H}_\tau^{Se} e^{-j\beta r_1}$. If one were to reduce the surface integral (6) to a contour integral, the final expression should contain only the edge field values. It is not possible to get an exact solution; however, an approximate solution can be obtained. The change of variable $u = \left(r_1 - r_R\right)$ is introduced and $\mathcal{J}_H$ can now be written as

$$\mathcal{J}_H = -\frac{e^{-j\beta(R_0+\vec{r}_{10}\cdot\hat{R}+u_l)}}{R_0} \int_0^{+\infty} \tilde{H}_\tau^{Se} e^{-j\beta u} \frac{((u+u_l)^2+\rho^2)}{2(u+u_l)^2} du \tag{7}$$

Here, u_l corresponds to the point Q_{RC} and H_τ^{Se} is a function of $(u+u_l)$. Using integration by parts, $\mathcal{J}_H$ can be expanded as follows:

$$\mathcal{J}_H = \mathcal{J}_{Ha} - \frac{e^{-j\beta(R_0+\vec{r}_{10}\bullet\hat{R})}}{R_0} \int_0^{+\infty} \frac{e^{-j\beta u}}{j\beta} \frac{d}{du}\left(\tilde{H}_\tau^{Se} \frac{((u+u_l)^2+\rho^2)}{2(u+u_l)^2} \right) du \tag{8}$$

where

$$\mathcal{J}_{Ha} = \frac{e^{-j\beta(R_0+\vec{r}_{10}\bullet\hat{R})}}{R_0} \left(\frac{(u_l^2+\rho^2)}{j2\beta u_l^2} \right) H_\tau^{Se} e^{j\beta u_l} \tag{9}$$

At this point, we will approximate $\mathcal{J}_H$, assuming it is equal to $\mathcal{J}_{Ha}$, which is evaluated along the contour and it is expressed in terms of the *R*-component of the magnetic field. The lower limit u_l of (9) depends on the position of the original sources inside the virtual surface. However, in a practical problem, the locations of the original sources inside the enclosed surface are not known and the only known quantity is the H_τ^S component on the contour. Therefore, one has to determine u_l or the term in the bracket of $\mathcal{J}_{Ha}$ from the H_τ^S component. It is observed in (3) and (4) that an approximation of this term can be obtained from the phase of the magnetic field on the contour. The derivation of the phase with respect to dr_R for large $\beta r_1, r_1 \gg \lambda/2$, is as follows.

$$\frac{\left(u_l^2+\rho^2\right)}{j2\beta u_l^2} = C_h \approx \left[\frac{d}{dr_R} Arg\left\{H_\tau^S\right\} + j\beta \right]_{u=0}^{-1} \tag{10}$$

In order to evaluate the accuracy of the approximate solution, we first solve for (7) using Fourier transform with respect to *u*. The integral of (7) can be represented as:

$$\int_{-\infty}^{+\infty} \upsilon(u) \frac{((u+u_l)^2+\rho^2)}{2(u+u_l)^2} \tilde{H}_\tau^{Se}(u+u_l) e^{-j\beta u} \; du = \left(\pi\delta(\beta) + \frac{1}{j\beta} \right) \otimes \mathbb{F}\left(\frac{((u+u_l)^2+\rho^2)}{2(u+u_l)^2} \tilde{H}_\tau^{Se}(u+u_l) \right) \tag{11}$$

where $\upsilon(u)$ is the unit step function. The derivation of an analytical expression for the error is extremely difficult, thus we have used a numerical approach. The results were obtained from Matlab simulations using Fast Fourier Transform (FFT) of $\mathcal{J}_H$. The above derivations are for the *H* field. The same approximation holds for the *E* filed. The relative error due to the approximation is given in Fig. 2. The results show the most significant field components only.

The approximate far field can now be expressed in mathematical form using (1), (8) and (10) as:

$$\vec{E} \approx -j\omega \iint_{S_{los}} \left(\hat{n}\times\vec{H}^S\right) \frac{e^{-j\beta R}}{R} ds + \frac{1}{4\pi} \oint_c \left(\hat{R}\times\hat{n}\right) H_\tau^S \frac{e^{-j\beta R}}{R} C_h dl - j\omega\eta \iint_{S_{los}} \left(\hat{R}\times\left(\hat{n}\times\vec{E}^S\right)\right) \frac{e^{-j\beta R}}{R} ds - \frac{\eta}{4\pi} \oint_c \hat{n} E_R^S \frac{e^{-j\beta R}}{R} C_h dl \tag{12}$$

The LoS approach can be further simplified under the condition that the LoS surface is smooth and that the observation point falls in the positive side of the unit normal for every surface point. Then, in (12), one can resolve either the surface integral over the equivalent electric currents ($2\hat{n}\times\vec{H}^S$) or the surface integral over the equivalent magnetic currents ($2\hat{n}\times\vec{E}^S$).

RESULTS AND DISCUSSION

In the LoS approach, two critical approximations were made; one is the on the phase term of the *H* field on the contour, and the other one is the substitution of $\mathcal{J}_H$ with $\mathcal{J}_{Ha}$. The first approximation sets the limit on the minimum size for the virtual surface; the distance between the surface and sources has to be greater than half a wavelength. In contrast, the second approximation sets the upper limit on the size of the virtual surface and this can be observed on the error plots of Fig2. The plots show that for a given ρ and β, the error increases as the distance r_R is increased. This is more pronounced in the approximation of the *E* field. However, an error of less than 5% is acceptable for most practical problems. Furthermore, as the virtual surface becomes large, the edge effects become negligible compared to the LoS contribution, thus the upper limit may not have significant effect on the overall accuracy.

The effectiveness of the LoS approach to the equivalence principle is demonstrated via the simulation of a 1/2λ dipole antenna. The dipole antenna is enclosed in a rectangular box of size 2λ×2λ×2.5λ, and the box is discretized with the number of cells set as 60×60×120. In order to observe only the effect of the LoS approach, the fields on the surface are calculated using (4) and (5). Once the surface fields are calculated, the surface currents are obtained from them, and the far field radiation pattern is calculated using (12). The simulation results of the radiation pattern in the far zone for the E_θ component in the *E*-plane with two different conditions are shown in Fig. 3. The two conditions are: (1) the radiation pattern using the standard equivalence principle, (2) the radiation pattern using the LoS approach. The physical size of the box for the simulation is such that the shortest distance between the antenna element and the surface of the box is 0.75λ, for which the maximum error is estimated to be within 5%. In the plots, the error below the relative gain of –15dB is attributed not to the approximation, but to the numerical errors. The simulation results show remarkable agreement between the LoS approach and the standard equivalence method.

In this paper, we have presented a new approach to the equivalence principle. The computation time for the LoS approach is roughly one sixth of the time required by the standard equivalence. Thus, the LoS approach can be an efficient algorithm for the computation of far field patterns in high-frequency structure simulators and the associated CAD tools.

REFERENCES

[1] J.A. Stratton, *Electromagnetic Theory,* New York: McGraw Hill, 1941.

[2] R. F. Harrington, *Time-Harmonic Electromagnetic Fields*, New York: McGraw Hill, 1961.

[3] C.A. Balanis, *Advanced Engineering Electromagnetic*, New York: John Wiley & Sons, 1989.

[4] A. Rubinowicz, "The Miyamoto-Wolf diffraction wave," *Progress in Optics,* vol.4, pp. 201-240, 1965.

[5] F. Kottler, "Diffraction at a black screen, part 2: Electromagnetic theory," *Progress in Optics*, vol.6, pp. 335-377, 1967.

[6] Ken-ichi Sakina, Suomin Cui and Makoto Ando, "Mathematical investigation of modified edge representation," *IEEE Antenna and Propagation Symposium*, Vol.1, pp. 386-389. 2000.

[7] John Asvestas, "The physical optics fields of an aperture on a perfectly conducting screen in terms of line integrals," *IEEE Trans. Antenna and Propagation*, Vol. AP-34 pp. 1155-1159. 1986.

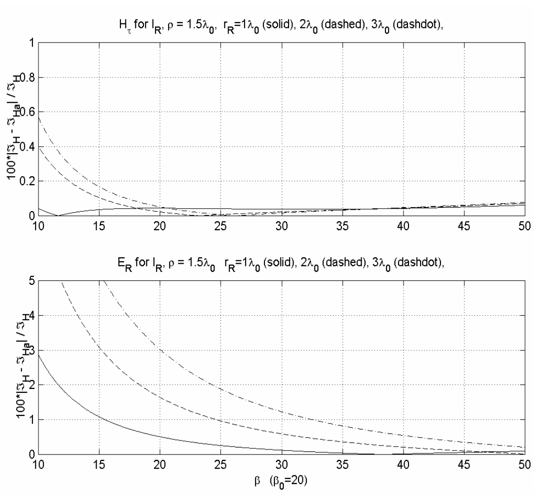

Fig. 2. Percentage error for *E* and *H* field.

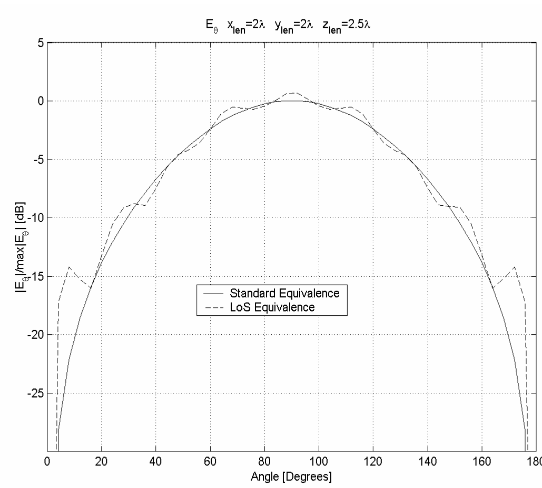

Fig. 3. E_θ component radiation pattern of a dipole antenna.